Method Article

Integrative programming for simulation of packaging headspace and shelf life of fresh produce

Ali Jalali, Manfred Linke, Martin Geyer, Pramod Mahajan*

Department of Horticultural Engineering, Leibniz Institute for Agricultural Engineering and Bioeconomy (ATB), Potsdam, Germany

A B S T R A C T

Fresh horticultural products are exposed to different environmental conditions from farm to fork. Barrier properties of packaging and physiological behaviour of produce, namely respiration and transpiration can affect headspace conditions surrounding produce and consequently remaining shelf life. Packaging material also plays a role in heat and mass transfer, such as thermal conduction and permeation of O_2, CO_2 and water vapour. All of these behaviours are integrated together in the form of ordinary differential equations and solved using numerical methods in MATLAB.

• The simulation program is useful for designing the size and number of perforations to achieve equilibrium modified atmosphere alone or in combination with packaging material having a higher water transmission rate or active moisture absorber.

• The simulation program is also useful for predicting the shelf life of fresh produce under the actual supply chain conditions.

• The simulation program provides a flexible system to input predefined supply chain conditions and the properties of fresh produce and packaging material, thus, minimizing the costly and time consuming experimental procedures for selecting the optimum packaging material for fresh produce.

© 2021 The Authors. Published by Elsevier B.V.
This is an open access article under the CC BY-NC-ND license
(http://creativecommons.org/licenses/by-nc-nd/4.0/)

---

* Corresponding author.
  E-mail address: pmahajan@atb-potsdam.de (P. Mahajan).

Specifications table

Subject Area	Agricultural and Biological Sciences
More specific subject area	Food Engineering
	Horticultural Technology
	Chemical and Process Engineering
Method name	Integrative programming for simulation of packaged fresh produce
Name and reference of original method	The code presented in this paper implements integrative mathematical modelling to simulate the effect of environmental conditions including temperature, relative humidity and gas composition on physiological behaviour of packaged fresh horticultural produce and predict headspace conditions, including gas composition, humidity and moisture condensation, mass loss and shelf life. The computational methods are inspired by the literature and primarily:
	• JALALI, A., LINKE, M., GEYER, M. & MAHAJAN, P. V. 2020. Shelf life prediction model for strawberry based on respiration and transpiration processes. Food Packaging and Shelf Life, 25, 100525.
	• JALALI, A., RUX, G., LINKE, M., GEYER, M., PANT, A., SAENGERLAUB, S. & MAHAJAN, P. 2019. Application of humidity absorbing trays to fresh produce packaging: Mathematical modelling and experimental validation. Journal of Food Engineering, 244, 115-125.
	• JALALI, A., SEIIEDLOU, S., LINKE, M. & MAHAJAN, P. 2017. A comprehensive simulation program for modified atmosphere and humidity packaging (MAHP) of fresh fruits and vegetables. Journal of Food Engineering, 206, 88-97.
	• Mahajan, P., Oliveira, F., Montanez, J. & Frias, J. 2007. Development of user-friendly software for design of modified atmosphere packaging for fresh and fresh-cut produce. Innov. Food Science & Emerging Technologies, 8, 84-92.
	• Hertog M, Boerrigter H, Van den Boogaard G, Tijskens L, Van Schaik A. 1999. Predicting keeping quality of strawberries (cv. Elsanta') packed under modified atmospheres: an integrated model approach. Postharvest Biology and Technology, 15(1): 1-12.
Resource availability	MATLAB code (www.mathworks.com) was written and a MATLAB code script file has been created.

Method description

This method aims to simulate the interaction between respiration and transpiration of produce, behaviour of packaging material such as permeability to gases and water vapour as well as moisture absorption and the ambient conditions such as temperature, relative humidity (RH) and gas composition in order to predict in package conditions such as gas composition, RH and moisture condensation [2,5,14], and finally quality and shelf life of packaged produce.

Fig. 1 shows the produce-packaging system including a respiring fresh horticultural produce such as strawberries in a closed plastic package covered with lidding perforated film. The produce consumes O_2 and produces CO_2 because of respiration, and releases water vapour to the surrounding area due to the transpiration process. Gases and water vapour can permeate in/out through the packaging film. Respiration also releases heat from the fruit surface to the packaging headspace. Packaging film and tray also exchange heat with the ambient atmosphere when there is a thermal gradient due to ongoing heat and mass transfer processes. There is also a potential of gas transmission across the film and its micro-perforations and moisture absorption by absorbing material embedded in packaging tray or sachets inside the tray. These assumptions and relevant mathematical formulation are discussed in more detail in previous publications [5,6,8,13]. Further details on modelling the effect of respiration and transpiration on shelf life of fresh produce are discussed in Jalali et al. [4].

Numerical simulation

Input variables to the mathematical modelling program cover produce properties, package properties and environmental conditions. These inputs provide initial and fixed values for the mathematical program to solve time dependent ordinary differential equations (ODEs) defining the physiological behaviour of fresh produce and heat and mass transfer phenomena which occur within
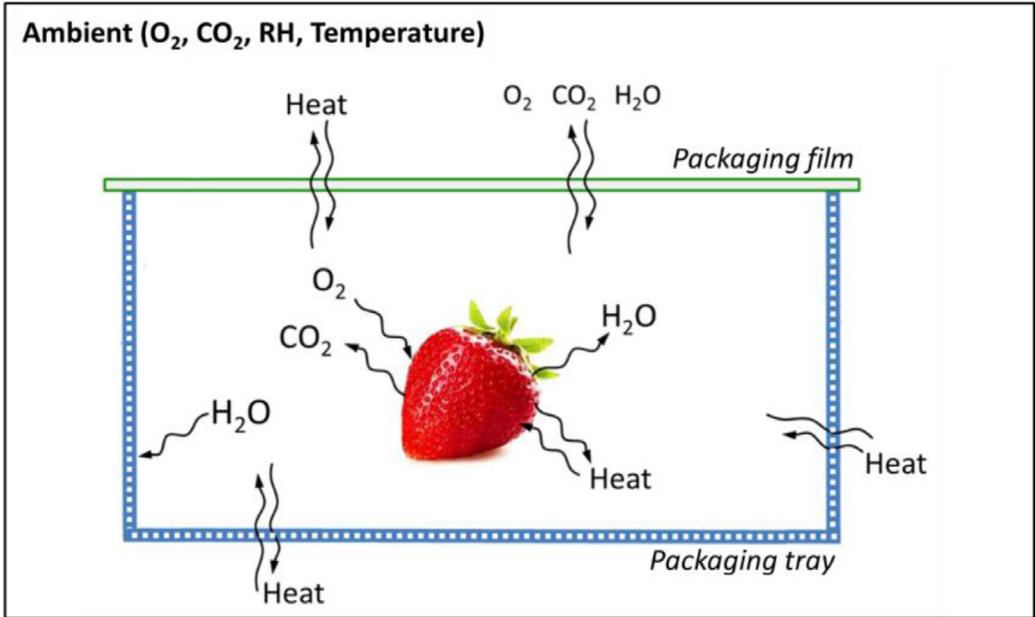
Fig. 1. Packaging-ambient system including fresh produce packaged and stored under given ambient conditions.

the packaging and surrounding atmosphere. All these variables and ODEs were integrated into a computer simulation program based on MATLAB software (MATLAB R2010b, MathWorks®, USA). ODEs with the general form $dy/dt = f(t, y)$ were solved numerically using Euler's method which is a first order Runge-Kutta method for numerical integration of ODEs, to predict output variables. In this method, given (initial) value (y_i) at time t_i, the value of the equation after one time step (dt) is approximated as $y_{i+1} = y_i + f(t_i, y_i)\ dt$ (Fig. 2). The simulation program was divided into 5 different modules namely gas concentration, humidity and condensation, fruit mass loss, microbial deterioration and shelf life and temperature, which were solved in that sequence with an iterative step of 1 second.

Table 1 shows the MATLAB script including the modelling duration and time interval, produce and packaging properties, and environmental conditions, defining the initial values to solve ODEs over the modelling duration. This script can be directly used in MATLAB or modified with user defined input parameters.

Module 1: Packaging gas concentration

The respiration rate of produce and permeation rate of packaging film O_2 and CO_2 are included in mass balance equations for headspace gases, which determine the equilibrium gas composition as expressed in Eqs. (1) and (2) respectively.

$$\frac{d\gamma_{O_2}^{in}}{dt} = \frac{\frac{dV_{O_2}^p}{dt} + \frac{dV_{O_2}^r}{dt}}{10^6 V_f} = \frac{\left[K_{O_2} A + \frac{10^6 N_p \pi R_p^2 D_{O_2}}{e + R_p} \right] \left(\gamma_{O_2}^{out} - \gamma_{O_2}^{in} \right) - \frac{W_p R_{O_2}}{\rho_{O_2}}}{10^6 V_f} \tag{1}$$

$$\frac{d\gamma_{CO_2}^{in}}{dt} = \frac{\frac{dV_{CO_2}^p}{dt} + \frac{dV_{CO_2}^r}{dt}}{10^6 V_f} = \frac{\left[K_{CO_2} A + \frac{10^6 N_p \pi R_p^2 D_{CO_2}}{e + R_p} \right] \left(\gamma_{CO_2}^{out} - \gamma_{CO_2}^{in} \right) + \frac{W_p R_{CO_2}}{\rho_{CO_2}}}{10^6 V_f} \tag{2}$$
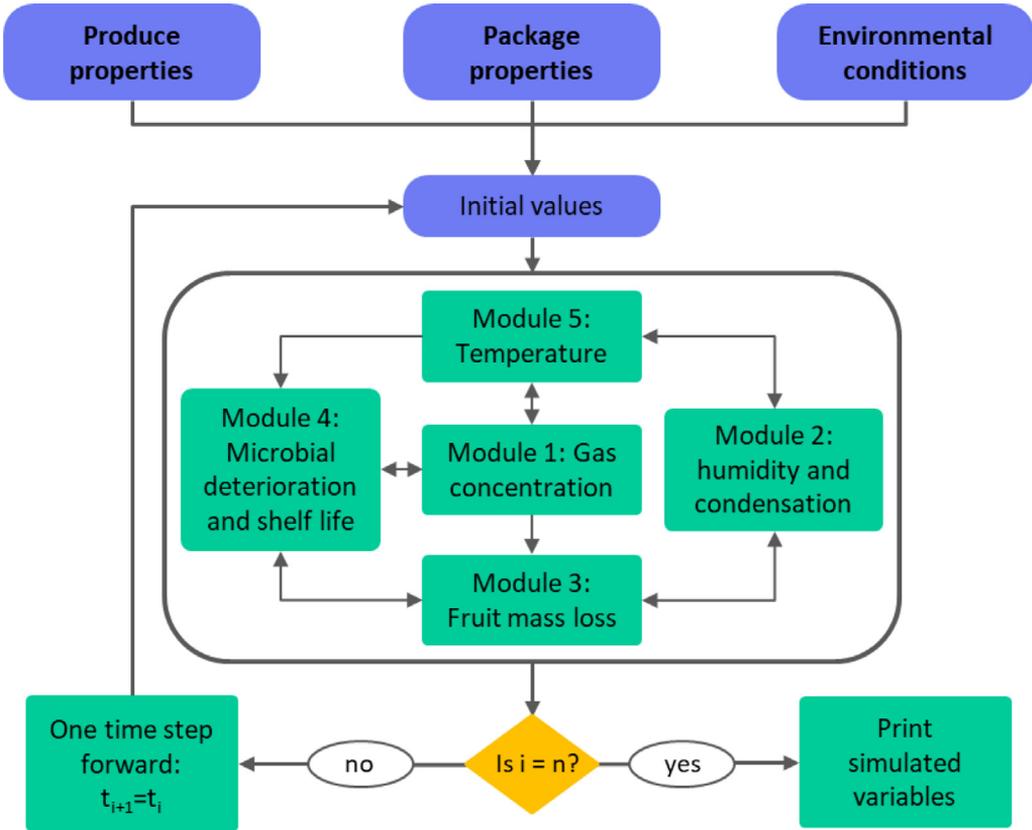
Fig. 2. Steps to follow integration and simulation of package headspace and shelf life. The symbols t, i and n stand for the time, the current time step number and the final time step number, respectively.

Where R_i is the respiration rate of O_2 consumption and CO_2 production (ml kg^{-1}h^{-1}) respectively, which are functions of temperature and atmosphere composition as presented in Eqs. (3) and (4) reported by Hertog et al. [3] for strawberries.

$$R_{O_2} = \frac{\gamma_{O_2}^{in}}{K_{mO_2} + \gamma_{O_2}^{in}} Vm_{O_2}^{ref} \; e^{\frac{E_{aO_2}}{R}\left[\frac{1}{T_{ref}} - \frac{1}{T}\right]} \tag{3}$$

$$R_{CO_2} = RQ_{ox}R_{O_2} + \frac{1}{\left(1 + \gamma_{O_2}^{in}/K_{mCO_2(f)}\right) + 1} Vm_{CO_2(f)}^{ref} e^{\frac{E_{aCO_2(f)}}{R}\left[\frac{1}{T_{ref}} - \frac{1}{T_i}\right]} \tag{4}$$

This module consists of basic aspects of physiological parameters that are also needed in all subsequent modules. This was because the interaction between different modules is a complex system. For example, the respiration will affect the surface temperature of fruit and thereby affects the transpiration and so on. Fig. 3 shows the simulation results for modified atmosphere packaging (MAP) of strawberries with one perforation of 1 mm, containing 400 g fruit stored in two different ambient temperatures of 10°C and 20°C. The results show the effect of temperature on equilibrium gas composition of MAP headspace, so that increasing temperature provides a bigger difference of gas concentration compared to normal air, due to a higher respiration rate.

Table 1

Basic inputs to integrative mathematical model.

```
clc,clear
D=2;            %(Experiment duration, days
dur=D*24;       %(Experiment duration, hours)
t=1/3600;       %(Time interval, hours)
NS=dur/t;       %(Number of steps)

% PRODUCT PROPERTIES (related to strawberry MAP)
Wp=0.4;     %(Product mass, kg)
np=14;      %(Product number)
Cp=3722.1;      %(specific heat of fresh produce, J/(kg.K))
Vp=(1.098*Wp*1000-0.39)*10^-6;      %(Fruit volume, m3)
dp=2*(3*Vp/(4*np*pi))^(1/3);            %(Fruit average radius, m)
As=(1.862*Wp*1000+10.650)*10^-4;        %(Overall surface area of fruits, m2)

% PACKAGE PROPERTIES
Wt=0.03;        %(Packaging tray mass, kg)
x=0.001;        %(Tray wall thickness, m)
e=100*10^-6;    %(Film thickness, m)
Po2ref=19*10^-6;%(Coefficient of permeability of film to O2, mg/(m2.h))
Pco2ref=76*10^-6;%(Coefficient of permeability of film to CO2, mg/(m2.h))
WVPref=26*10^-5;%(Permeability of film to water vapour, mg/(m2.h.Pa))
Kt=0.19*3600;   %(thermal conductivity of polyethylene, j/(h.m.K))
Ct=1670;        %(specific heat of plastic, j/(kg.K))
Dp=0.003;       %(Radius of the perforation, m)
Np=1;           %(Number of film perforations)
W=0.105;        %(width package assumed as horizontal plate, m)
L=0.128;        %(length package assumed as horizontal plate, m)
D=0.07;         %(Depth of package assumed as vertical plate)
Ap1=L*W;        %(surface area of top of package, m2)
Ap1=L*W;        %(surface area of bottom of package, m2)
Ap2=D*(W+L+W+L);%(surface area of sides as symmetrical trapezoids, m2)
Ap=2*Ap1+Ap2;   %(surface area of package, m2)
A=Ap1;          %(Breathable film area, m^2)
Vt=W*L*D;       %(Total package volume, m3)
Vf=Vt-Vp;       %(Package free volume, Cubic meter)

% ENVIRONMENTAL CONDITIONS
Tout=20;        %(Ambient temperature, C)
RHout=50;       %(Ambient relative humidity, %)
yo2out=20.9;    %(Outside O2 concentration, percent)
yco2out=0.03;   %(Outside CO2 concentration, percent)
%% Initial values
T(1)=Tout(1);   %(Initial headspace temperature, C)
Ts(1)=Tout(1);  %(Initial fruit surface temperature, C)
Tt(1)=Tout(1);  %(Initial package tray wall temperature, C)
RH(1)=RHout(1);     %(Initial headspace relative humidity, %)
yo2(1)=yo2out(1); %(Initial O2 concentration, percent)
yco2(1)=yco2out(1); %(Initial CO2 concentration, percent)
Mtr(1)=0;       %(Initial total moisture transpiration, mg)
Mfilm(1)=0;     %(Initial total moisture permeation, mg)
Mabsorb(1)=0;   %(Initial total moisture transpiration, mg)
Mloss(1)=0;     %(Initial total oxidative mass loss, mg)
MlossT(1)=0;    %(Initial total fruit mass loss, mg)
Det(1)=0.27;        %(Initial total microbial deterioration, %)
```

Module 2: Packaging humidity and condensation

The mass balance of total moisture in the package is presented in Eq. (5) [4], where the rate of total moisture change (dM_t/dt) depends on the rate of moisture transpiration by produce (dM_{tr}/dt), permeation through packaging film (dM_f/dt) and perforations and absorption by packaging tray (dM_a/dt).

$$\frac{dM_t}{dt} = \frac{dM_{tr}}{dt} - \frac{dM_f}{dt} - \frac{dM_{ab}}{dt} \tag{5}$$

Moisture loss rate by produce depends on the transpiration rate, as a function of vapour pressure deficit (VPD) between the produce surface and headspace air, as well as the mass transfer coefficient for produce skin (K_s) and thin air layer (K_a) (mg m^{-2}h^{-1}Pa^{-1}). VPD itself is generated when there is either difference between the water activity of produce and headspace RH, or a temperature difference

Table 2
Code implementation for module 1: Packaging gas concentration.

```
kmo2=2.63;        %(Michaelis-Menten constant, Percent)
vmo2ref=0.27;      %(Max O2 consumption rate at reference Temp, micromole/kg.S)
Eavmo2=74826;    %(O2 respiration activation energy, J/mol)
RQ=0.91;          %(Respiratory quotient)
kmco2f=0.056;    %(Michaelis-Menten constant, Percent)
vmco2fref=0.50;  %(Max CO2 production rate at reference Temp, micromole/kg.S)
Eavmco2f=57374;  %(CO2 respiration activation energy, J/mol)
Do2=0.073;        %(Diffusion coefficient of O2 in air) m2/h
Dco2=0.0742;      %(Diffusion coefficient of CO2 in air, m2/h)
Tref=10;          %(Reference temperature, C)
R=8.314472;       %(Gas constant, J/mol.K)

    for i=1:NS
    %% Module 1: Packaging gas concentration
    Densityo2(i)=(1.429-0.0049*T(i));
    Ro2(i)=yo2(i)/(kmo2+yo2(i))*vmo2ref*exp((Eavmo2/R)*(1/(Tref+273.15)-...
        1/(Ts(i)+273.15)))*(32*3.6);
    dVo2p(i)=t*(Po2ref/e*A+(10^6*pi*(Dp/2)^2*Do2*Np/(e+(Dp/2))))*...
        (yo2out/100-yo2(i)/100);
    dVo2r(i)=-Wp*t*Ro2(i)/Densityo2(i);
    dVo2(i)=dVo2p(i)+dVo2r(i);
    dyo2(i)=dVo2(i)*10^-6/Vf*100;
    yo2(i+1)=yo2(i)+dyo2(i);
    % CO2
    Densityco2(i)=(1.977-0.0068*T(i));
    Rco2(i)=(44*3.6)*(RQ*Ro2(i)/(32*3.6)+(1/(1+yo2(i)/kmco2f+1))*...
        vmco2fref*exp((Eavmco2f/R)*(1/(Tref+273.15)-1/(Ts(i)+273.15))));
    dVco2p(i)=t*(Pco2ref/e*A+(10^6*pi*(Dp/2)^2*Dco2*Np/(e+(Dp/2))))*...
        (yco2out/100-yco2(i)/100);
    dVco2r(i)=Wp*t*Rco2(i)/Densityco2(i);
    dVco2(i)=dVco2p(i)+dVco2r(i);
    dyco2(i)=dVco2(i)*10^-6/Vf*100;
    yco2(i+1)=yco2(i)+dyco2(i);
    %% Module 2: Packaging humidity and condensation
    %% Module 3: Fruit mass loss
    %% Module 4: Microbial deterioration and shelf life
    %% Module 5: Temperature
    End
                        %OUTPUT VISUALIZATION
figure(3)
xaxisdiv=12;xaxislable='Time (h)';
plot(yo2,'LineWidth',2),hold on,plot(yco2,'g--','LineWidth',2)
legend('O_2','CO_2');
xlabel(xaxislable,'fontsize',14);ylabel('Gas Concentration(%)','fontsize',14);
set(gca,'XTick',0:xaxisdiv:t:NS,'XTickLabel',{0:xaxisdiv:NS*t},'fontsize',16,'XLim',[0 NS]);
```
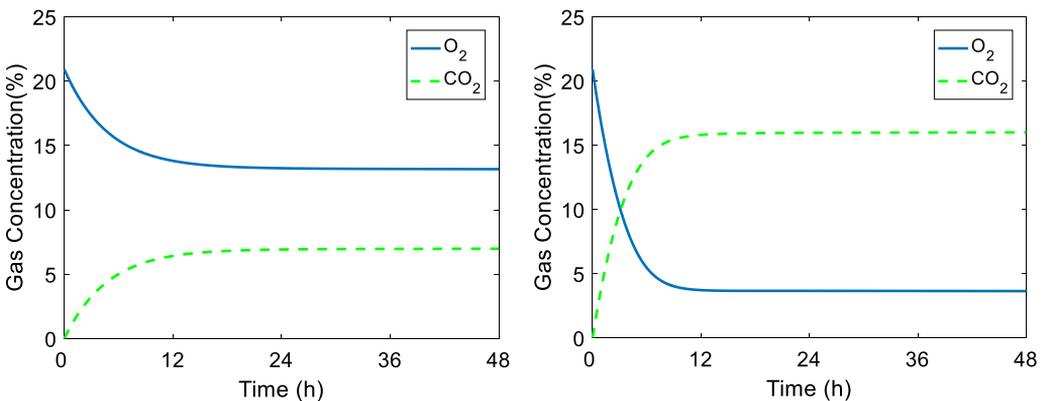

Fig. 3. Equilibrium gas composition of headspace for a strawberry package with one perforation of 1 mm diameter in the film under 10℃ (left) and 20℃ (right) storage temperature.

Table 3

Code implementation for module 2: Packaging humidity and moisture condensation.

```
Patm=1.01325*10^5;%(Atmospheric Pressure, Pa)
Rd=287.058;      %(Specific gas constant for dry air, 287.058 J/(kg·K)
Rv=461.495;      %(Specific gas constant for water vapor, 461.495 J/(kg·K)
awi=0.99;  %(Water activity on fruit surface: 0-1)
Ks=13.6*10^-3*3600;  %(Fruit skin mass transfer coefficient, mg/(m2.h.Pa))
MMh2o=0.018016; %Molar mass of water vapor, 0.018016 kg/mol)
Babsorb=11.4;
MMdair=0.028964;    %(Molar mass of dry air, 0.028964 kg/mol)

    %% Module 1: Packaging gas concentration
    %% Module 2: Packaging humidity and condensation
    for i=1:NS
    % Psychrometry
    Lv(i)=(2502535.259-2385.76424*T(i))*10^-6;  %(Latent heat of vaporisation, j/mg)
    Dair(i)=Patm/(287.05*(T(i)+273.15));    %(Density of air, kg/m3)%
    Psat(i)=610.94*exp(17.625*T(i)/(243.04+T(i)));  %(Water vapour saturation pressure in
    headspace, Pa)%
    Psats(i)=610.94*exp(17.625*Ts(i)/(243.04+Ts(i)));   %(Water vapour saturation pressure,
    Pa)%
    Psatout(i)=610.94*exp(17.625*Tout(1)/(243.04+Tout(1))); %(Water vapour saturation
    pressure in ambient, Pa)%
    Pin(1)=RH(1)/100*Psat(1);    %(Water vapour partial pressure, Pa)%
    Pdair(i)=Patm-Pin(i);   %(Dry air partial pressure, Pa)%
    Dairhumid(i)=Pdair(i)/(Rd*(T(i)+273.15))+Pin(i)/(Rv*(T(i)+273.15));%(Density of humid
    air, kg/m3)
    Wa(i)=Vf*Dairhumid(i);  %(Mass of headspace air, kg)
    Mairmax(i)=0.002166*Psat(i)/(T(i)+273.16)*Vf*10^6;  %(Max. moisture content of headspace
    air, kg)
    Mtotal(1)=0.002166*Pin(1)/(T(1)+273.16)*Vf*10^6;    %(initial moisture in packaging free
    space kg)
    Mair(1)=Mtotal(1);  %(initial moisture content of headspace air, kg)
    % Moisture condensation and relative humidity
    if Mtotal(i)>Mairmax(i)
        Mcond(i+1)=Mtotal(i)-Mairmax(i);Mair(i)=Mairmax(i);
    else
        Mcond(i+1)=0;Mair(i)=Mtotal(i);
    end
    dMcond(i)=Mcond(i+1)-Mcond(i);
    RH(i)=100*(Patm/Psat(i))*(Mair(i)*10^-3/(0.622*(Dairhumid(i)*1000*Vf)...
        +Mair(i)*10^-3));
    % Moisture transpiration
    Dv(i)=9.1*10^-9*((T(i)+273.15)^2.5)/((T(i)+273.15)+245.18)*3600;     %(Diffusivity of
    water vapor in air (m2/h))
    Ka(i)=2*Dv(i)/((T(i)+273.15)*dp*(R/MMh2o))*10^6*3600/1;     %(Thin air layer mass
    transfer coefficient, mg/(m2.h.Pa))
    Ps(i)=awi*Psats(i);      %(Water vapor pressure on fruit surface, Pa)
    VPD(i)=Ps(i)-Pin(i);   %(Vapor Pressure Deficit, Pa)
    dMtr(i)=t*As*VPD(i)/(1/Ks+1/Ka(i));
    if dMtr(i)<0
    dMtr(i)=0;
    end
    Mtr(i+1)=Mtr(i)+dMtr(i);
    % Moisture absorption
    Mabsorbeq(i)=0.057*exp(0.057*RH(i))-Mabsorb(i)/1000;
    dMabsorb(i)=0*Mabsorbeq(i)*(1-exp((-t/24)/Babsorb))*1000;
    Mabsorb(i+1)=Mabsorb(i)+dMabsorb(i);
    % Moisture permeation
    Pin(i)=(Psat(i)*RH(i)/100);
    Pout(i)=(Psatout(i)*RHout(1)/100);
    Dwv(i)=Dair(i)*(1+Mair(i)*10^-3/Wa(i))/(1+MMdair/MMh2o*Mair(i)*10^-3/Wa(i));
    dMfilm(i)=Dwv(i)*t*(WVPref/e*A+(10^6*pi*(Dp/2)^2*Dv(i)*Np/(e+(Dp/2))))*Dwv(i)*(RH(i)/100-
    RHout(1)/100)*Psat(i)/(R/MMh2o*(T(i)+273.15));
    Mfilm(i+1)=Mfilm(i)+dMfilm(i);
    % Final moistures
    dMtotal(i)=dMtr(i)-dMabsorb(i)-dMfilm(i);
    Mtotal(i+1)=Mtotal(i)+dMtotal(i);
    if Mtotal(i+1)>Mairmax(i)
        Mair(i+1)=Mairmax(i);
    else
        Mair(i+1)=Mtotal(i);
    end
    Pin(i+1)=Mair(i+1)/(Vf*10^6)*(T(i)+273.16)/0.002166;
    %% Module 3: Fruit mass loss
    %% Module 4: Microbial deterioration and shelf life
    %% Module 5: Temperature
    end



                            %OUTPUT VISUALIZATION
figure(4)
xaxisdiv=12;xaxislable='Time (h)';
plot(Mtr*10^-3,'LineWidth',2),hold on,plot(Mabsorb*10^-3,'r','LineWidth',2),plot(Mcond*10^-
3,'g','LineWidth',2),plot(Mfilm*10^-3,'k','LineWidth',2)
legend('Moisture loss','Absorption','Condensation','Permeation','Total mass loss','Ox. mass
loss','Location','northwest')
xlabel(xaxislable,'fontsize',14);ylabel('Mass (g)','fontsize',14);
set(gca,'XTick',0:xaxisdiv/t:NS,'XTickLabel',{0:xaxisdiv:NS*t},'fontsize',16,'XLim',[0
NS],'YLim',[0 4]);

figure(5)
plot(RH,'LineWidth',2)
xlabel(xaxislable,'fontsize',14);ylabel('Relative Humidity (%)','fontsize',14);
set(gca,'XTick',0:xaxisdiv/t:NS);set(gca,'XTickLabel',{0:xaxisdiv:NS*t},'fontsize',16);
set(gca,'XTick',0:xaxisdiv/t:NS,'XTickLabel',{0:xaxisdiv:NS*t},'fontsize',16,'XLim',[0 NS]);
```

Table 4

Code implementation for module 3: Fruit mass loss.

```
    for i=1:NS
    %% Module 1: Packaging gas concentration
    %% Module 2: Packaging humidity and condensation
    %% Module 3: Fruit mass loss
    % Oxidative mass loss
    dMloss(i)=Rco2(i)*Wp*t*(180-108)/264;
    Mloss(i+1)=Mloss(i)+dMloss(i);
    % Total mass loss
    MlossT(i)=Mloss(i)+Mtr(i);
    %% Module 4: Microbial deterioration and shelf life
    %% Module 5: Temperature
    end
                            %OUTPUT VISUALIZATION
figure(6)
xaxisdiv=12;xaxislable='Time (h)';
plot(MlossT*10^-6/Wp*100,'LineWidth',2),hold on,plot(Mloss*10^-
6/Wp*100,'r','LineWidth',2),plot(Mtr*10^-6/Wp*100,'g','LineWidth',2)
legend('Total mass loss','Ox. mass loss','Moisture loss','Location','northwest')
xlabel(xaxislable,'fontsize',14);ylabel('Loss (%)','fontsize',14);
set(gca,'XTick',0:xaxisdiv/t:NS,'XTickLabel',{0:xaxisdiv:NS*t},'fontsize',16,'XLim',[0
NS],'YLim',[0 1]);
```

Table 5

Code implementation for module 4: Microbial deterioration and shelf life.

```
Det_max=13;          %(Maximum acceptable total microbial deterioration, %)
yco2max=30;      %Maximal CO2 (%) withstanding by microorganisms

    for i=1:NS
    %% Module 1: Packaging gas concentration
    %% Module 2: Packaging humidity and condensation
    %% Module 3: Fruit mass loss
    %% Module 4: Microbial deterioration and shelf life
    %(Deterioration, %)
    Ksp(i)=(3e-6*log(T(i))+2e-6)*3600;          %(Spoilage constant  h^-1)
    co2_rel(i)=1-yco2(i)/yco2max;            %(Deterioration inhibition parameter)
    dDet(i)=t*Ksp(i)*Det(i)*((100-Det(i))/100)*co2_rel(i);
    Det(i+1)=Det(i)+dDet(i);
    %(Keeping quality (shelf life under given conditions))
    if Det(i)<=Det_max
        KQ(i)=i;
    else
        KQ(i)=0;
    end
    %% Module 5: Temperature
    end
                            %OUTPUT VISUALIZATION
figure(7)
xaxisdiv=12;xaxislable='Time (h)';
plot(Det,'LineWidth',2),hold on
xlabel(xaxislable,'fontsize',14);ylabel('Deterioration (%)','fontsize',14);
MaxKQ=max(KQ);
line([0 NS],[Det_max Det_max],'color',[0 0 0],'LineStyle','-','LineWidth',0.5)
line([MaxKQ MaxKQ],[0 Det_max],'color',[0 0 0],'LineStyle','--','LineWidth',0.5)
annotation(figure(5),'textbox',[0.19 0.67 0.28 0.05],'String','Acceptance
limit','LineStyle','none','FontSize',14,'FitBoxToText','off');
annotation(figure(5),'textbox',[0.67 0.24 0.16 0.05],'String','Shelf
life','LineStyle','none','FontSize',14,'FitBoxToText','off');
set(gca,'XTick',0:xaxisdiv/t:NS,'XTickLabel',{0:xaxisdiv:NS*t},'fontsize',16,'XLim',[0
NS],'YLim',[0 20])
```

between the surface and headspace air (Eq. (6)).

$$\frac{dM_{tr}}{dt} = A_s \frac{d_{tr}}{dt} = A_s \frac{VPD}{\left(\frac{1}{K_s} + \frac{1}{K_a}\right)} = A_s \frac{P_s^{sat} a_w - P_{in}^{sat} RH_{in}/100}{\left(\frac{1}{K_s} + \frac{1}{K_a}\right)} \tag{6}$$

The total moisture permeation rate through packaging film and perforations is a function of film permeability to water vapour, the size and number of perforations as well as the vapour pressure

Table 6
Code implementation for module 5: Temperature.

```
Mu=1.87e-5;      %(Dynamic viscosity, Pa.s=kg/(m.s2))
k=0.027;         %(Thermal conductivity of air, W/(m.K)=J/(s.m.K))
g=9.81;     %(gravitational acceleration, m/s2)

    for i=1:NS
    %% Module 1: Packaging gas concentration
    %% Module 2: Packaging humidity and condensation
    %% Module 3: Fruit mass loss
    %% Module 4: Microbial deterioration and shelf life
    %% Module 5: Temperature
    % convective heat transfer coefficient for packaging tray
    Ca(i)=(1.005+1.82*Mair(i)*10^-6/(Vf*Dairhumid(i)))*10^3;      %(Humid heat of air,
    J/kg.K)
    beta1(i)=1/((T(i)+Tt(i))/2+273.15);
    %(Grashof number for top, bottom and side wall)
    Grtop(i)=L^3*Dairhumid(i)^2*g*abs(T(i)-Tt(i))*beta1(i)/Mu^2;
    Grbott(i)=L^3*Dairhumid(i)^2*g*abs(T(i)-Tt(i))*beta1(i)/Mu^2;
    Grside(i)=D^3*Dairhumid(i)^2*g*abs(T(i)-Tt(i))*beta1(i)/Mu^2;
    Pr(i)=Mu*Ca(i)/k;        %Prandtl number
    %(Rayleigh number for top, bottom and side wall)
    Ratop(i)=Grtop(i)*Pr(i);
    Rabott(i)=Grbott(i)*Pr(i);
    Raside(i)=Grside(i)*Pr(i);
    %(Nusselt number for top, bottom and side wall)
    if Tt(i)<T(i)
        Nutop(i)=0.54*Ratop(i)^0.25;Nubott(i)=0.27*Rabott(i)^(1/3);
    else
        Nutop(i)=0.27*Ratop(i)^(1/3);Nubott(i)=0.54*Rabott(i)^0.25;
    end
    Nuside(i)=(0.825+(0.387*Raside(i)^(1/6)/((1+(0.492/Pr(i))^(9/16))^(8/27))))^2;
    %(For all values of Ra)
    %(heat transfer coefficient (W/(m2.K)for top, bottom and side wall)
    hptop(i)=3600*k/L*Nutop(i);
    hpbott(i)=3600*k/L*Nubott(i);
    hpside(i)=3600*k/D*Nuside(i);
    hp(i)=1*(Ap1*hptop(i)+Ap1*hpbott(i)+Ap2*hpside(i))/Ap; %(Average heat transfer
    coefficient (W/(m2.K))
    % convective heat transfer coefficient for fruit
    beta2(i)=1/((T(i)+Ts(i))/2+273.15);
    Gr(i)=dp^3*Dairhumid(i)^2*g*abs(T(i)-Ts(i))*beta2(i)/Mu^2;%Grashof number)
    Pr(i)=Mu*Ca(i)/k;        %(Prandtl number)
    Ra(i)=Gr(i)*Pr(i);       %(Rayleigh number)
    Nu(i)=(2+0.589*Ra(i)^0.25/(1+(0.469/Pr(i))^(9/16))^(4/9));      %(Nusselt number)
    hs(i)=1*3600*k*Nu(i)/dp;        %(heat transfer coefficient, W/(m2.K))
    % final temperatures
    %(Tray wall)
    dTt(i)=(t*((Kt*Ap*(Tout(1)-Tt(i))/x)+hp(i)*Ap*(T(i)-Tt(i))+(dMabsorb(i)-
    dMfilm(i)+dMcond(i))*Lv(i)))/(Wt*Ct);
    Tt(i+1)=Tt(i)+dTt(i);
    %(Fruit surface)
    dTs(i)=(t*(Wp*Rco2(i)*6.21+hs(i)*As*(T(i)-Ts(i)))-(dMtr(i))*Lv(i))/(Wp*Cp);
    Ts(i+1)=Ts(i)+dTs(i);
    %(Headspace air)
    dT(i)=(t*(hp(i)*Ap*(Tt(i)-T(i))-hs(i)*As*(T(i)-Ts(i)))+(dMtotal(i))*Lv(i))/(Wa(i)*Ca(i));
    T(i+1)=T(i)+dT(i);
    end
                          %OUTPUT VISUALIZATION
figure(8)
xaxisdiv=12;xaxislable='Time (h)';
plot(T,'LineWidth',2),hold
on,plot(Ts,'r','LineWidth',2),plot(Tt,'g','LineWidth',2),plot(Tout,'k','LineWidth',2)
legend('T_{in}','T_{fruit surface}','T_{tray wall}','T_{out}','Location','northwest')
xlabel(xaxislable,'fontsize',14);ylabel('Temperature (°C)','fontsize',14);
set(gca,'XTick',0:xaxisdiv/t:NS);set(gca,'XTickLabel',{0:xaxisdiv:NS*t},'fontsize',16);
set(gca,'XTick',0:xaxisdiv/t:NS,'XTickLabel',{0:xaxisdiv:NS*t},'fontsize',16,'XLim',[0
NS],'YLim',[Tout(1) Tout(1)+2]);
```

gradient between headspace and ambient air as presented in Eq. (7).

$$\frac{dM_f}{dt} = \rho_{wv}\left[K_{H_2O}A + \frac{10^6 N_p \pi R_p^2 D_{H_2O}}{e + R_p}\right]\left(\frac{RH_{out} - RH_{in}}{100}\right)\frac{P_{in}^{sat}}{R(T + 273.15)} \tag{7}$$
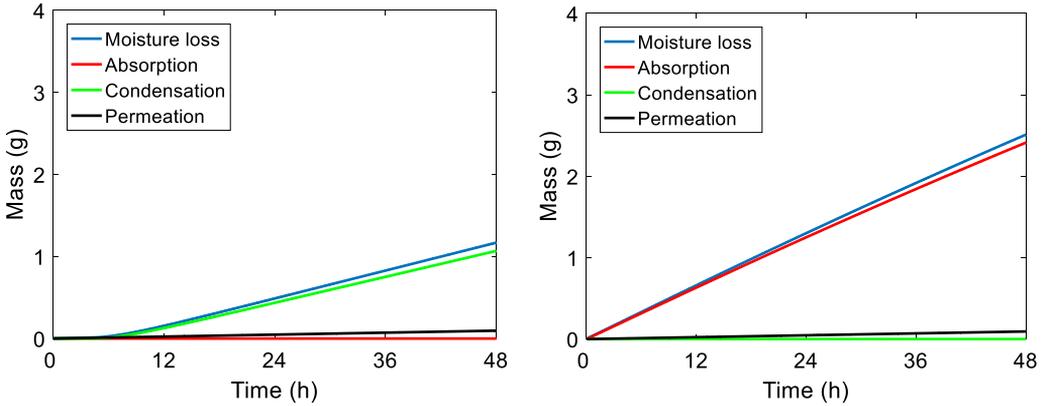
Fig. 4. Moisture distribution for strawberry packaged in the normal plastic tray (left) and moisture absorber tray (right) under 20°C storage temperature.

Eq. (8) represents a Weibull type moisture absorption rate for humidity packaging trays reported by Rux et al. [11] and Jalali et al. [5].

$$\frac{dM_{ab}}{dt} = 10^3 M_{eq} e^{\left(\frac{-t}{24 \, \beta}\right)} \tag{8}$$

In Eq. (8), the moisture absorption capacity at equilibrium, M_{eq} is a function of RH in packaging headspace [5,13]. Integration of Eq. (9) against time gives the cumulative moisture within the package. The difference between the cumulative moisture and maximum moisture holding capacity of air at each temperature determined the total condensation ($M_c = M_t - M_{a.max}$), while the total moisture present in headspace air is the difference between cumulative moisture and cumulative condensation ($M_a = M_t - M_c$), so that until there is no water condensed, the air moisture would be equal to cumulative moisture. The RH of headspace is then calculated as a function of headspace air moisture based on psychometric rules [1] as expressed in Eq. (9).

$$RH_{in} = 100 \times \frac{P_{atm} \times \frac{M_a \times 10^{-3}}{W_{air}}}{P_{sat}\left(0.622 + \frac{M_a \times 10^{-3}}{W_{air}}\right)} \tag{9}$$

Fig. 4 shows the evolution of different moisture components over the simulation time for a normal plastic tray and a moisture absorber tray under 20°C storage temperature. Both packages had a perforation of 3 mm diameter in packaging film. Results showed that most of the transpired moisture from fruit was condensed in the normal plastic package. Moisture absorber in a package could prevent condensation by absorbing the excess water, however, imposed a higher total moisture transpiration compared to the normal plastic package. This was due to moisture absorption decreases vapor pressure in packaging headspace, which is compensated by more transpiration consequently. Fig. 5 shows the headspace RH of both packaging types. RH in the moisture absorbing tray was only slightly less than the normal plastic tray. This was also due to the higher transpiration of fruit in the moisture absorbing tray, which prevented the decrease in RH.

Module 3: Fruit mass loss

Fruit mass loss (as a percentage compared to initial mass) calculated as one of the quality indices was used to predict the shelf life of fresh produce during the supply chain. Mass loss based shelf life is the time it takes to reach the maximum acceptable mass loss (MAM) as a percent of initial fruit mass and was determined 4.3% for strawberries [4]. It is separated into two different parts. The first part was moisture loss due to fruit transpiration and the second part was due to oxidative mass
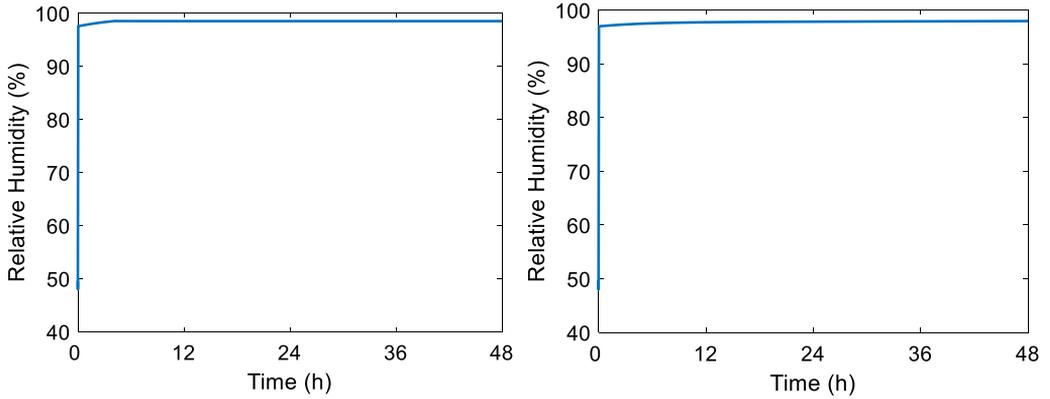
Fig. 5. Headspace RH for strawberry packaged in the normal plastic tray (left) and moisture absorber tray (right) under 20°C storage temperature.
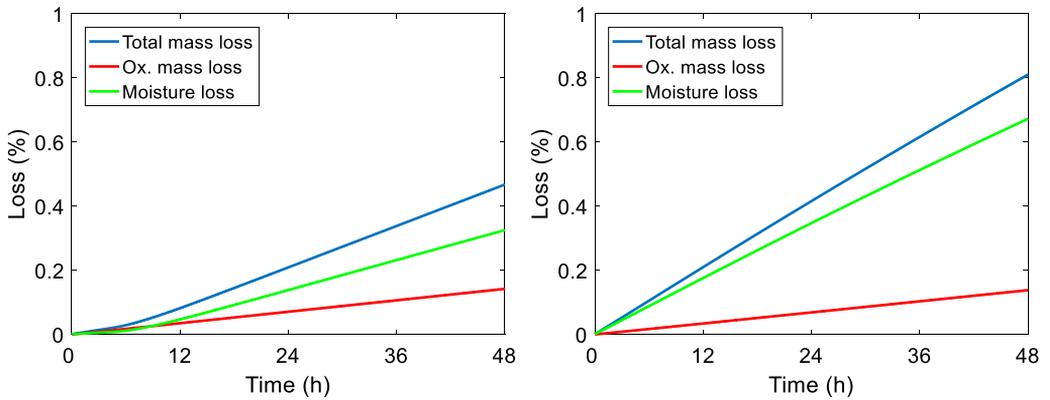
Fig. 6. Percentage mass loss components for strawberry packaged in the normal plastic tray (left) and moisture absorber tray (right) under 20°C storage temperature.

loss resulting from fruit respiration. The overall equation for the oxidation of glucose as the substrate for aerobic respiration is $C_6H_{12}O_6 + 6\ O_2 \rightarrow 6\ CO_2 + 6\ H_2O + $ energy. Then for respiratory oxidation of 180 g (1 mole) of glucose, 192 g (6 moles) of O_2 is consumed which diffuses into the tissue from the surrounding atmosphere, while 264g (6 moles) of CO_2 diffuses out. The 108 g (6 moles) of H_2O produced is simply incorporated into the aqueous solution of the cell [7]. Hence the total mass loss (dL_t/dt) was estimated as the sum of mass loss from respiratory oxidation of the substrate (dL_{ox}/dt) [6] and moisture loss due to transpiration (Eq. (5)).

$$\frac{dL_{ox}}{dt} = W_p R_{CO_2} (180 - 108)/264 \tag{10}$$

$$\frac{dL_t}{dt} = \frac{dM_{ox}}{dt} + \frac{dM_{tr}}{dt} \tag{11}$$

Fig. 6 shows the simulation results of fruit mass loss and its components for strawberry packages with the same conditions as the previous section. Oxidative mass loss is almost the same for both packages as it changes with storage temperature. Total mass loss in moisture absorber package was higher than the normal plastic package, since higher transpiration rate imposed by moisture absorption.
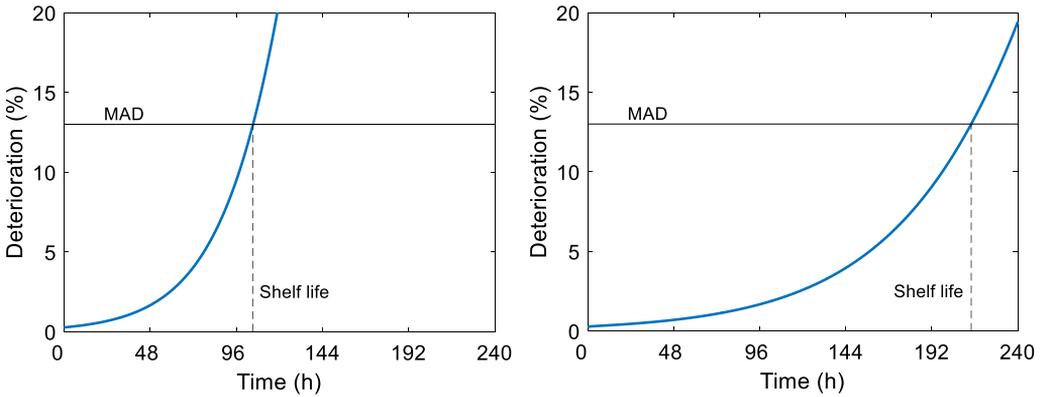
Fig. 7. Microbial deterioration for strawberry package in (left) non-MAP (19.5% O_2 & 1.2% CO_2) and (right) MAP (3.5% O_2 & 16.1% CO_2) stored under 20℃.

Module 4: Microbial deterioration and shelf life

Microbial deterioration was another quality index to predict the shelf life of fresh produce. Deterioration based shelf life is the time it takes the produce to reach the maximum acceptable deterioration (MAD) as a percentage. Matar et al. [10] provided a mathematical model to predict fungal decay for packaged strawberries Eq. (12) and ((13)), where they defined 13% of visible deterioration as MAD, using a global visual method for measuring the deterioration of strawberries in MAP [9].

$$\frac{dN}{dt} = K_d N \frac{N_{max} - N}{N_{max}} CO_{2_{rel}} \qquad (12)$$

$$CO_{2_{rel}} = 1 - \frac{y_{CO_2}}{y_{CO_2}^{max}} \qquad (13)$$

Where deterioration constant, K_d is a function of temperature and metabolic rate, $CO_{2_{rel}}$ is a deterioration-inhibiting factor due to CO_2 evolution.

The effect of two different packaging types, including non-MAP (19.5% O_2 & 1.2% CO_2 at equilibrium) made by 20 perforations of 1 mm diameter in packaging film and MAP (3.5% O_2 & 16.1% CO_2 at equilibrium) made by one perforation of 1 mm diameter in the film is showed in Fig. 7. Lower respiration of fruit under MAP conditions led to a lower deterioration rate, thereby, increased the shelf life to 214 h compared to 105 h under non-MAP conditions.

Module 5: Temperature

Thermal equilibrium equations were used to calculate steady-state heat and mass transfer to predict the temperature changes on produce surface, headspace air, internal and external tray and film surface according to changes in ambient temperature. Thermal equilibrium between produce and headspace air is a balance between rates of internal heat production due to respiration, convective heat transferred from headspace air to produce surface. Eq. (14) is based on the thermal equilibrium between produce surface and headspace air to calculate the rate of surface temperature change [12].

$$\frac{dT_s}{dt} = \frac{6.21 \, R_{CO_2} W_p - \frac{dM_{tr}}{dt}\lambda + h_s A_s (T_i - T_s)}{W_p C_p} \qquad (14)$$

In a similar way, the rate of temperature change on the internal surface of the packaging tray was calculated from the thermal equilibrium between headspace air and the inner surface of the tray and
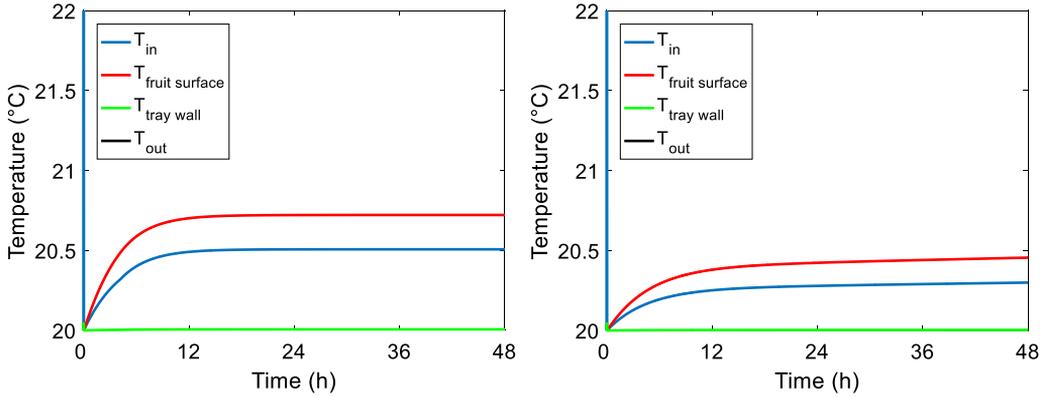
Fig. 8. Temperature evolution for strawberry packaged in the normal plastic tray (left) moisture absorber tray (right) under 20°C storage temperature.

film (Eq. (15)).

$$\frac{dT_t}{dt} = \frac{\frac{K_t A_t (T_o - T_t)}{x} - h_t A_t (T_i - T_t) + \left(\frac{dM_{ab}}{dt} + \frac{dM_c}{dt} - \frac{dM_f}{dt}\right)\lambda}{W_t C_t} \tag{15}$$

In addition, the overall thermal equilibrium inside the package used to calculate the rate of temperature change in headspace air.

$$\frac{dT_i}{dt} = \frac{h_t A_t (T_t - T_i) - h_s A_s (T_i - T_s) + \frac{dM_t}{dt}\lambda}{W_a C_a} \tag{16}$$

Fig. 8 shows temperature evolution for packaging tray wall, headspace and fruit surface for normal plastic and moisture absorber tray packaging under 20°C. As the moisture absorbing tray led to a higher transpiration rate of fruit, the cooling effect of moisture evaporation from the fruit surface led to a lower fruit surface and consequently headspace air temperature in this package compared to normal plastic tray packaging. Internal tray wall temperature was very slightly higher than the ambient air temperature, which was not visible, so that tray wall temperature fitted on the ambient temperature curve.

Method application under realistic supply chain conditions

The ultimate objective of the integrating simulation program was to provide flexibility to adapt to varying supply chain conditions of fresh horticultural produce, therefore, optimization of packaging material. Fig. 9 shows an example of a typical supply chain of harvested strawberries, in which fluctuating conditions fitting different postharvest processes served as simulation input in order to compare keeping quality of fruit under different postharvest chain scenarios including MAP and open tray packaging [4]. Under the identical supply chain conditions, MAP showed different packaging headspace temperature and RH compared to the open tray packaging where the fruits are exposed directly to the ambient conditions of the supply chain (Fig. 9).

Fig. 10 shows the effect of different packaging types on the shelf life of fresh strawberries under the same supply chain conditions. The values for using MAP, it was possible to delay the microbial deterioration and percentage mass loss to meet the maximum acceptable value for about 2.5 d and 1 d, respectively rather than open tray packaging. However, both cases showed that the shelf life was limited by the percentage mass loss, as it reached the maximum acceptable value in a shorter time compared to the microbial deterioration. The integrating simulation program, thus, was a useful
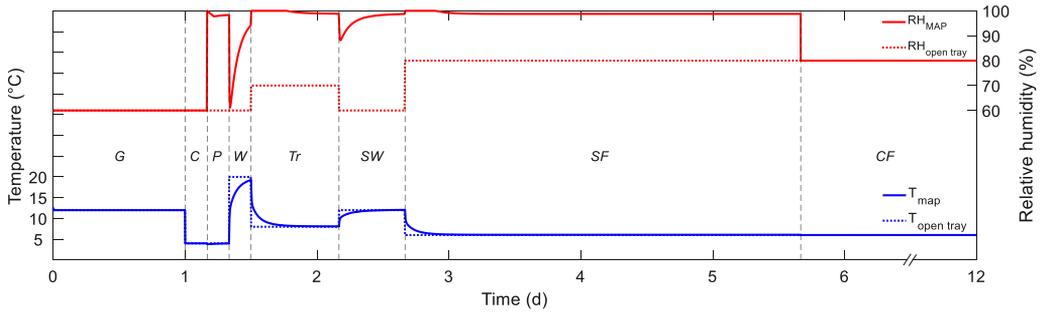
Fig. 9. Supply chain profile for postharvest handling of fresh strawberries under MAP and open tray packaging conditions (total time subdivisions: Grower (G), Cooling (C), Packaging (P), Wholesale (W), Transport (Tr), Supermarket Warehouse (SW), Supermarket Fridge (SF) and Consumer Fridge (CF)).
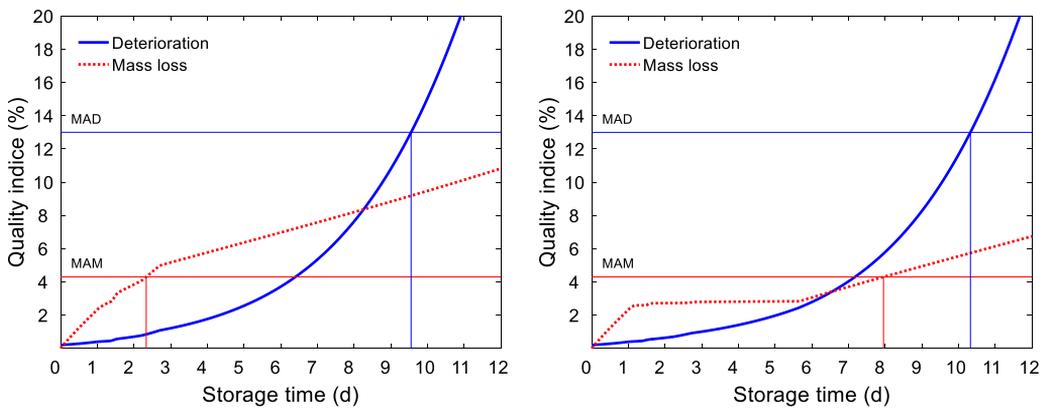
Fig. 10. The effect of open tray packaging (left) and MAP conditions (right) on different quality indices (percentage mass loss and percentage microbial deterioration under realistic supply chain conditions).

tool for the design and optimization of packaging for fresh produce under dynamically changing environmental conditions.

Declaration of Competing Interest

The authors declare that they have no known competing financial interests or personal relationships that could have appeared to influence the work reported in this paper.

Acknowledgements

Supplementary materials

Supplementary material associated with this article (MATLAB .m file) can be found, in the online version, at doi:10.1016/j.mex.2021.101514.

References

[1] Ashrae, A.H.F. 1997. American Society of Heating. *Refrigeration and Air Conditioning Engineers*.

[2] S. Fishman, V. Rodov, S. Ben-Yehoshua, Mathematical model for perforation effect on oxygen and water vapor dynamics in modified-atmosphere packages, J. Food Sci. 61 (1996) 956–961.

[3] M. Hertog, H. Boerrigter, G. Van Den Boogaard, L. Tijskens, A. Van Schaik, Predicting keeping quality of strawberries (cv.Elsanta') packed under modified atmospheres: an integrated model approach, Postharvest Biol. Technol. 15 (1999) 1–12.

[4] A. Jalali, M. Linke, M. Geyer, P.V Mahajan, Shelf life prediction model for strawberry based on respiration and transpiration processes, Food Packag. Shelf Life 25 (2020) 100525.

[5] A. Jalali, G. Rux, M. Linke, M. Geyer, A. Pant, S. Saengerlaub, P. Mahajan, Application of humidity absorbing trays to fresh produce packaging: mathematical modeling and experimental validation, J. Food Eng. 244 (2019) 115–125.

[6] A. Jalali, S. Seiiedlou, M. Linke, P. Mahajan, A comprehensive simulation program for modified atmosphere and humidity packaging (MAHP) of fresh fruits and vegetables, J. Food Eng. 206 (2017) 88–97.

[7] A.A. Kader, M.E Saltveit, Respiration and gas exchange, Postharvest Physiol. Pathol. Veg. 2 (2003) 7–29.

[8] P. Mahajan, F. Oliveira, J. Montanez, J. Frias, Development of user-friendly software for design of modified atmosphere packaging for fresh and fresh-cut produce, Innovative Food Sci. Emerg. Technol. 8 (2007) 84–92.

[9] C. Matar, S. Gaucel, N. Gontard, S. Guilbert, V. Guillard, A global visual method for measuring the deterioration of strawberries in MAP, MethodsX 5 (2018) 944–949.

[10] C. Matar, S. Gaucel, N. Gontard, S. Guilbert, V. Guillard, Predicting shelf life gain of fresh strawberries 'Charlotte cv'in modified atmosphere packaging, Postharvest Biol. Technol. 142 (2018) 28–38.

[11] G. Rux, P.V. Mahajan, M. Linke, A. Pant, S. Sängerlaub, O.J. Caleb, M Geyer, Humidity-regulating trays: moisture absorption kinetics and applications for fresh produce packaging, Food Bioprocess Technol. (2016) 1–8.

[12] Y. Song, N. Vorsa, K.L Yam, Modeling respiration–transpiration in a modified atmosphere packaging system containing blueberry, J. Food Eng. 53 (2002) 103–109.

[13] M.J. Sousa-Gallagher, P.V Mahajan, Integrative mathematical modelling for MAP design of fresh-produce: theoretical analysis and experimental validation, Food Control 29 (2013) 444–450.

[14] G. Xanthopoulos, E. Koronaki, A. Boudouvis, Mass transport analysis in perforation-mediated modified atmosphere packaging of strawberries, J. Food Eng. 111 (2012) 326–335.